2014 IEEE International Conference on Robotics & Automation (ICRA)
Hong Kong Convention and Exhibition Center
May 31 - June 7, 2014. Hong Kong, China

Single Beacon based Multi-Robot Cooperative Localization using Moving Horizon Estimation

Sen Wang, Ling Chen, Dongbing Gu and Huosheng Hu

Abstract— **This paper studies three-dimensional multi-robot Cooperative Localization (CL) problem. Most of existing CL strategies adopt Extended Kalman Filter (EKF) or Maximum a Posteriori (MAP). In this paper, a novel approach based on Moving Horizon Estimation (MHE) is proposed. The main contribution of this paper is twofold: 1) MHE is integrated with EKF for three-dimensional CL using single mobile beacon, which can bound localization error, impose various constraints on states and noises, and make use of previous range measurements for current estimation. 2) A sufficient condition on observability of multi-robot CL is derived by using Fisher Information Matrix. Simulation is conducted to verify that the proposed MHE based CL algorithm outperforms EKF based method in terms of localization accuracy, and two scenarios where our algorithm is superior to EKF are discussed.**

I. INTRODUCTION

Recently, multi-robot cooperative system is in high demand to accomplish various complex tasks. Localization which provides pose estimate for robot is a prerequisite for multi-robot cooperation. Multi-robot Cooperative Localization (CL) is to localize a group of robots and improve their estimated positions by sharing information and using relative measurements, which benefits both the group and each individual robot [1].

To address multi-robot CL problem, various state estimation methods have been adopted. Extended Kalman filter (EKF) is the approach receiving most interest owing to its ease of use and low computational complexity. In [1], a distributed EKF algorithm which decomposes the estimation to different robots is proposed. In [2], all the robots exchange their states with each other to derive a global estimate by EKF. EKF based CL using various relative observations [3], EKF consistency based CL [4], etc. are also studied. Although EKF is a classic solution for CL, it is a filter rather than smoother and the linearization of nonlinear system may cause estimator inconsistency and big linearization errors [4]. Particle Filter (PF) method which is applicable to nonlinear system can be employed, see [5]. A drawback of PF is computational complexity.

Maximum Likelihood Estimation (MLE) is also suitable for CL problem with nonlinear models [6]. However, MLE ignores prior probability, which is important for robot localization. Maximum a Posteriori (MAP) based approach can overcome this disadvantage of MLE, and also improve the localization accuracy by both employing the nonlinear system models and smoothing the estimate over the state trajectory [7]. However, the computational complexity of MAP grows over time since all the previous states and observed measurements are involved in the optimization, making it unsuitable for real-time applications. In [8], [9], a sliding window filter is used for stereo vision and simultaneous localization and mapping, respectively, to bound the computation complexity by marginalization. However, none of these algorithms considers the importance of constraints which are imposed on states and noises by physical systems. In [10], Moving Horizon Estimation (MHE) is designed for a two-dimensional localization problem with the aid of several static beacons. Recently, we proposed a MHE based three-dimensional localization algorithm for robot using single beacon [11], whereas no work has been carried out on MHE based multi-robot CL.

In order to bound the localization error, the system is required to be observable. In [4], [12], the rank of observability matrix is proposed for observability analysis of robot localization systems with linear or linearized nonlinear models. However, the original systems are usually nonlinear and the linearization may cause the incorrect decision on observability [13]. Therefore, the observability rank condition derived from Lie derivative for nonlinear system is used in [13], [14]. However, all these studies transform discrete time systems into continuous-time systems under the assumption that sample time is sufficiently small. A straightforward method which is able to directly analyze the observability of discrete-time localization system is proposed in [11]. For observability analysis of fixed-window system, Fisher Information Matrix (FIM) technique can be applied [15], such as [16] using it for visual odometry.

In this paper, a novel MHE based CL algorithm is proposed as a superior alternative to the widely used EKF. The main contribution of this paper is twofold: 1) MHE based CL which provides bounded localization error and balances computational complexity and estimate accuracy is designed. It can incorporate physical constraints which are difficult to be introduced into EKF. The importance of constraint is examined by discussing two scenarios where our algorithm outperforms EKF based algorithm. 2) Based on the techniques used in [9], [15], [16], a sufficient condition on observability of MHE based CL is derived in the perspective of FIM.

The rest of this paper is organized as follows. Section II outlines the research problem. In Section III and IV, the proposed algorithm and FIM based observability analysis are provided respectively. Section V presents the simulation results. Finally, the conclusions are presented in Section VI.

The authors are with School of Computer Science and Electronic Engineering, University of Essex, Colchester CO4 3SQ, United Kingdom {swangi,lcheno,dgu,hhu}@essex.ac.uk

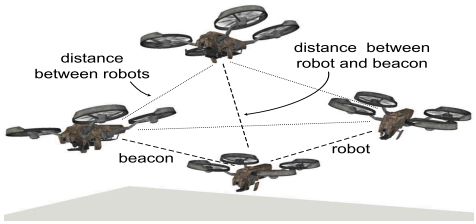

Fig. 1. Single beacon based multi-robot localization in three-dimension.

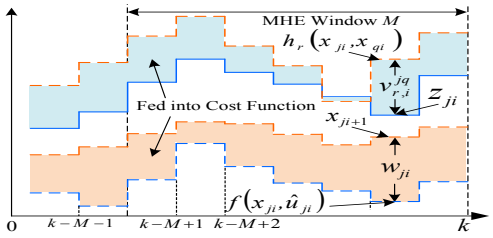

Fig. 2. Mechanism of MHE.

II. Cooperative Localization with Single Beacon

In this section, both multi-robot CL problem and system model are described.

A. Problem Description

In this CL system, there is a team of robots and a SMB cooperating with each other by flocking control [17], see Fig. 1. Each robot is equipped with proprioceptive sensors to perceive the linear velocity. An altitude sensor, an Inertial Measurement Unit (IMU) and a wireless sensor network (WSN) node are installed as exteroceptive devices. The SMB provides the reference position for the robots. Each robot can obtain the ranges to the other robots and SMB by WSN.

Suppose the state of N robots working cooperatively at time i is

$$\boldsymbol{x}_i = \begin{bmatrix} \boldsymbol{x}_{1_i}^T & \dots & \boldsymbol{x}_{j_i}^T & \dots & \boldsymbol{x}_{N_i}^T \end{bmatrix}^T \tag{1}$$

where $\boldsymbol{x}_{j_i} = [\boldsymbol{p}_{j_i}^T, \boldsymbol{\varphi}_{j_i}^T]^T = [x_{j_i}, y_{j_i}, z_{j_i}, \phi_{j_i}, \theta_{j_i}, \psi_{j_i}]^T$ is the pose (position $\boldsymbol{p}$ and orientation $\boldsymbol{\varphi}$) of the jth robot in three-dimension at time i. Throughout this paper, let $\hat{\boldsymbol{x}}_{j_i}$ denote the estimate of true state $\boldsymbol{x}_{j_i}$, and $\bar{\boldsymbol{x}} = \boldsymbol{x} - \hat{\boldsymbol{x}}$ denote the error between the true value and the estimate. The neighborhood set of robot j at time i, which comprises all its directly communicated robots and SMB, is represented as $\boldsymbol{N}_{j_i}$. Note that $\mathbf{0}$ and $\boldsymbol{I}$ denote the zero and identity matrices of compatible dimensions throughout this paper.

B. System Models

1) Process Model: The process model of the jth robot is

$$\boldsymbol{x}_{j_{i+1}} = f(\boldsymbol{x}_{j_i}, \hat{\boldsymbol{u}}_{j_i}, \boldsymbol{w}_{j_i}) \tag{2}$$

where $\hat{\boldsymbol{u}}_{j_i}$ is the measured motion vector of the robot between time i and $i+1$ with respect to the local frame of robot j at time i, and this control input is assumed to be affected by an additive Gaussian noise $\boldsymbol{w}_{j_i} \sim \mathcal{N}(0, \boldsymbol{Q}_{j_i})$. If some proprioceptive sensors are employed, such as a camera using optical flow, $\hat{\boldsymbol{u}}_{j_i}$ can be perceived. Otherwise, it is set as constant. Then, the motion model for the robot team is

$$\boldsymbol{x}_{i+1} = f(\boldsymbol{x}_i, \hat{\boldsymbol{u}}_i, \boldsymbol{w}_i) \tag{3}$$

where $\boldsymbol{w}_i \sim \mathcal{N}(0, \boldsymbol{Q}_i)$.

2) Measurement Models: The exteroceptive sensors are employed to refine the predicted estimate. The on-board IMU and altimeter are introduced to update the predicted attitude and altitude. Measurements between the robots, such as relative distance and/or bearing, are normally applied in CL to alleviate or bound the position uncertainty and error. In this work, a SMB is introduced. The measurement model for robot j at time i with three types of measurements is

$$\boldsymbol{z}_{j_i} = h(\boldsymbol{x}_{j_i}, \cdots, \boldsymbol{x}_{q_i}, \cdots) + \boldsymbol{v}_{j_i}, \quad q \in \boldsymbol{N}_{j_i} \tag{4}$$

where $\boldsymbol{v}_{j_i} \sim \mathcal{N}(0, \boldsymbol{R}_{j_i})$ is the Gaussian noise on measurement. The details of these measurements are below:

a) Range measurement: The beacon or robots share their information periodically via WSN for the other robots in neighbor to use and estimate the ranges between them. Denote the position of SMB at time i by $(x_{b_i}, y_{b_i}, z_{b_i})$. Then, the range measurements of robot j to robot q and SMB are

$$z_{r,i}^{jq} = h_r(\boldsymbol{x}_{j_i}, \boldsymbol{x}_{q_i}) + v_{r,i}^{jq}, \quad q \in \boldsymbol{N}_{j_i} \tag{5}$$

and

$$z_{r,i}^{jb} = h_r(\boldsymbol{x}_{j_i}, \boldsymbol{x}_{b_i}) + v_{r,i}^{jb}, \quad b \in \boldsymbol{N}_{j_i} \tag{6}$$

respectively. We denote ${}^{j}\boldsymbol{H}_{r,i}^{jq}$, ${}^{q}\boldsymbol{H}_{r,i}^{jq}$ and ${}^{j}\boldsymbol{H}_{r,i}^{jb}$ as the Jacobian matrices of these equations with respect to $\boldsymbol{x}_{j_i}$, $\boldsymbol{x}_{q_i}$ and $\boldsymbol{x}_{j_i}$ respectively, and $v_{r,i}^{jq} \sim \mathcal{N}(0, R_{r,i}^{jq})$ and $v_{r,i}^{jb} \sim \mathcal{N}(0, R_{r,i}^{jb})$.

b) Attitude measurement: The IMU observation which has already been fused with magnetometer is used to estimate the attitude by

$$\boldsymbol{z}_{a,i}^{j} = \boldsymbol{H}_{a,i}^{j}\boldsymbol{x}_{j_i} + \boldsymbol{v}_{a,i}^{j} = \begin{bmatrix} \mathbf{0} & \boldsymbol{I} \end{bmatrix} \boldsymbol{x}_{j_i} + \boldsymbol{v}_{a,i}^{j} \tag{7}$$

where $\boldsymbol{v}_{a,i}^{j} \sim \mathcal{N}(0, \boldsymbol{R}_{a,i}^{j})$. Note that the IMU is used as an exteroceptive sensor due to the presence of magnetometer.

c) Altitude measurement: The altitude measured by altimeter is

$$z_{d,i}^{j} = \boldsymbol{H}_{d,i}^{j}\boldsymbol{x}_{j_i} + v_{d,i}^{j} = \begin{bmatrix} 0 & 0 & 1 & \mathbf{0} \end{bmatrix} \boldsymbol{x}_{j_i} + v_{d,i}^{j} \tag{8}$$

with the variance $R_{d,i}^{j}$.

The SMB based multi-robot CL problem is how to simultaneously and accurately localize multiple robots modeled as (2) with the aid of the measurement model (4).

C. State Constraints

The prior knowledge of the system and the environment can be applied to constrain the states and noises, which can highly improve the algorithm performance. Suppose states, control inputs and noises satisfy the following constraints:

$$g_l(\boldsymbol{x}, \boldsymbol{u}, \boldsymbol{w}) \leq 0, \qquad l = 1, \cdots, m. \tag{9}$$

When performing the state estimation, these constraints should be taken into account to make sure the results are reasonable and accurate.

III. MHE BASED COOPERATIVE LOCALIZATION

MHE based CL is formulated into a fixed-window optimization incorporating constraints. It consists of two parts: EKF based dead-reckoning (DR) and MHE based update. EKF based DR calculates traveled displacement and changed orientation with respect to the previously estimated poses. The states evolved by DR are further fused with range measurements by MHE based update. This structure is able to free MHE from frequently updating the attitude and altitude measurements, whose sample rates are too high for MHE to handle since MHE requires relatively long time to solve the nonlinear optimization compared with EKF.

A. Dead-Reckoning

1) Prediction: State $\boldsymbol{x}$ is propagated by using model (3), and the covariance matrix $\boldsymbol{P}$ at time k is obtained by

$$\boldsymbol{P}_k = \boldsymbol{F}_k \boldsymbol{P}_{k-1} \boldsymbol{F}_k^T + \boldsymbol{G}_k \boldsymbol{Q}_k \boldsymbol{G}_k^T \tag{10}$$

where $\boldsymbol{F}_k$ and $\boldsymbol{G}_k$ are the Jacobian matrices of (3) with respect to $\boldsymbol{x}_k$ and $\boldsymbol{w}_k$ respectively. This prediction produces drifts over time due to the noise on the measured $\hat{\boldsymbol{u}}_{j_i}$.

2) Update using Attitude and Altitude Measurements: The IMU and altimeter are introduced to reduce the error accumulated by prediction. Because both these measurements can be acquired much faster than the range measurement, the prediction is updated by the attitude and altitude measurements at a high rate. Once an attitude or altitude measurement is received, a standard EKF is used to update their state mean and covariance using noise-free equations (7), (8) and (10). Technical details of EKF design for multiple robots are omitted here due to its straightforward steps. Please refer to [17] for more details.

B. MHE based Update using Range Measurement

When a range measurement is obtained, MHE based update is used to fuse the range and the position propagated by DR. Under the assumption that the robots are independent and the evolution of the state is a discrete-time Markov process, the positions of robots can be obtained by solving the following optimization problem [7]:

$$\begin{aligned}
&\underset{\boldsymbol{x}_0,\ldots,\boldsymbol{x}_k}{\operatorname{argmax}}\, p(\boldsymbol{x}_0, \boldsymbol{x}_1, \ldots, \boldsymbol{x}_k | \boldsymbol{z}_0, \boldsymbol{z}_1, \ldots, \boldsymbol{z}_k) \\
&= \underset{\boldsymbol{x}_0,\ldots,\boldsymbol{x}_k}{\operatorname{argmin}} \sum_{j=1}^{N} \|\boldsymbol{x}_{j_0} - \hat{\boldsymbol{x}}_{j_0}\|^2_{\boldsymbol{\Pi}_{j_0}^{-1}} + \sum_{i=0}^{k}\sum_{j=1}^{N} \|\boldsymbol{z}_{j_i} - h(\boldsymbol{x}_{j_i}, \ldots)\|^2_{\boldsymbol{R}_{j_i}^{-1}} \\
&+ \sum_{i=0}^{k-1}\sum_{j=1}^{N} \|\boldsymbol{x}_{j_{i+1}} - f(\boldsymbol{x}_{j_i}, \hat{\boldsymbol{u}}_{j_i})\|^2_{\boldsymbol{Q}_{j_i}^{-1}}
\end{aligned} \tag{11}$$

where $\|z\|_A^2 = z^T A z$, $N(\hat{\boldsymbol{x}}_{j_0}, \boldsymbol{\Pi}_{j_0})$ is prior knowledge on the initial state of robot j, and $\boldsymbol{z}_i$ is all the measurements at time i. Denote $\{\cdot\}_0^k$ as the set of states from time 0 to k. The aim of (11) is to optimally obtain all the poses of robots up to time k given all the control inputs $\{\hat{\boldsymbol{u}}_i\}_0^{k-1}$ and the measurements $\{\boldsymbol{z}_i\}_0^k$ from the beginning. Note that if (2) is linearized as $f(\boldsymbol{x}_{j_i}, \hat{\boldsymbol{u}}_{j_i}) + \boldsymbol{G}_{j_i}\boldsymbol{w}_{j_i}$, then $\boldsymbol{Q}_{j_i}$ should be replaced with $\boldsymbol{G}_{j_i}\boldsymbol{Q}_{j_i}\boldsymbol{G}_{j_i}^T$. The problem of (11) is that the computational complexity increases over time because all the previously calculated states and observed measurements are involved in the optimization. This hinders its use for long-term or real-time application.

In order to overcome this problem, a MHE method is adopted. (11) can be represented by separating the time interval into two sections $\{t : 0 \le t \le k-M-1\}$ and $\{t : k-M \le t \le k\}$ in the context of range measurement only:

$$\begin{aligned}
&\underset{\{\boldsymbol{x}_i\}_0^k}{\operatorname{argmin}} \sum_{i=k-M}^{k}\sum_{j=1}^{N}\sum_{q\in\boldsymbol{N}_{j_i}} \|\boldsymbol{z}_{r,i}^{jq} - h_r(\boldsymbol{x}_{j_i}, \boldsymbol{x}_{q_i})\|^2_{\boldsymbol{R}_i^{jq-1}} \\
&+ \sum_{i=k-M}^{k-1}\sum_{j=1}^{N} \|\boldsymbol{x}_{j_{i+1}} - f(\boldsymbol{x}_{j_i}, \hat{\boldsymbol{u}}_{j_i})\|^2_{\boldsymbol{Q}_{j_i}^{-1}} + \mathcal{Z}_{k-M}(\boldsymbol{x}_{k-M})
\end{aligned} \tag{12}$$

where

$$\begin{aligned}
\mathcal{Z}_{k-M}(\boldsymbol{x}_{k-M}) = &\sum_{i=0}^{k-M-1}\sum_{j=1}^{N}\sum_{q\in\boldsymbol{N}_{j_i}} \|\boldsymbol{z}_{r,i}^{jq} - h_r(\boldsymbol{x}_{j_i}, \boldsymbol{x}_{q_i})\|^2_{\boldsymbol{R}_i^{jq-1}} + \\
&\sum_{i=0}^{k-M-1}\sum_{j=1}^{N} \|\boldsymbol{x}_{j_{i+1}} - f(\boldsymbol{x}_{j_i}, \hat{\boldsymbol{u}}_{j_i})\|^2_{\boldsymbol{Q}_{j_i}^{-1}} + \sum_{j=1}^{N} \|\boldsymbol{x}_{j_0} - \hat{\boldsymbol{x}}_{j_0}\|^2_{\boldsymbol{\Pi}_{j_0}^{-1}}
\end{aligned} \tag{13}$$

is arrival cost of MHE, and M is the window size of MHE. Arrival cost is essential in MHE because it converts the originally unbounded optimization problem into a fixed size problem by summarizing the effect of observations $\{\boldsymbol{z}_i\}_0^{k-M-1}$ on $\boldsymbol{x}_{k-M}$. In order to compute $\mathcal{Z}_{k-M}(\boldsymbol{x}_{k-M})$ efficiently, it is better to have an algebraic expression for the arrival cost. Unfortunately, there is no exact algebraic expression of arrival cost for majority of systems, particularly when constraints are involved or the process model is nonlinear [18]. A solution to obtain an approximate algebraic expression is to use EKF covariance update recursively. Specifically, approximating the arrival cost uses

$$\hat{\mathcal{Z}}_{i+1}(\boldsymbol{x}_{i+1}) = \|\boldsymbol{x}_{i+1} - \hat{\boldsymbol{x}}_{i+1}\|^2_{\boldsymbol{P}_{i+1}^{-1}} \tag{14}$$

where

$$\boldsymbol{P}_{i+1} = \boldsymbol{G}_i\boldsymbol{Q}_i\boldsymbol{G}_i^T + \boldsymbol{F}_i(\boldsymbol{P}_i - \boldsymbol{P}_i\boldsymbol{H}_i^T(\boldsymbol{R}_i + \boldsymbol{H}_i\boldsymbol{P}_i\boldsymbol{H}_i^T)^{-1}\boldsymbol{H}_i\boldsymbol{P}_i)\boldsymbol{F}_i^T. \tag{15}$$

Therefore, MHE based CL can be formulated as

$$\begin{aligned}
&\underset{\{\boldsymbol{x}_i\}_{k-M}^k}{\operatorname{argmin}} \sum_{i=k-M}^{k}\sum_{j=1}^{N}\sum_{q\in\boldsymbol{N}_{j_i}} \|\boldsymbol{z}_{r,i}^{jq} - h_r(\boldsymbol{x}_{j_i}, \boldsymbol{x}_{q_i})\|^2_{\boldsymbol{R}_i^{jq-1}} \\
&+ \sum_{i=k-M}^{k-1}\sum_{j=1}^{N} \|\boldsymbol{x}_{j_{i+1}} - f(\boldsymbol{x}_{j_i}, \hat{\boldsymbol{u}}_{j_i})\|^2_{\boldsymbol{Q}_{j_i}^{-1}} + \hat{\mathcal{Z}}_{k-M}(\boldsymbol{x}_{k-M}) \\
&\textbf{s.t.} \qquad g_l(\boldsymbol{x}, \boldsymbol{u}, \boldsymbol{w}) \le 0, \qquad l = 1, \cdots, m
\end{aligned} \tag{16}$$

where $g_l(\boldsymbol{x}, \boldsymbol{u}, \boldsymbol{w}) \le 0$ are the various constraints on states and noises. To solve this optimization problem, the interior-point algorithm is employed with an initial guess given by DR. Then, current estimate $\boldsymbol{x}_k$ can be yielded by solving this optimization problem. The mechanism of MHE is shown in Fig. 2, where the shadowed areas are the cost trying to be minimized.

IV. FIM BASED OBSERVABILITY ANALYSIS

To successfully localize the robots with bounded uncertainty, all the states have to be observable with respect to the

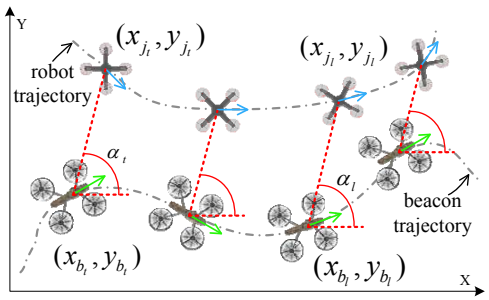

Fig. 3. A scenario where the system is unobservable. The relative directions α between robot and beacon remain constant during the period.

measurement model. Note that owing to the presence of IMU and altimeter, it is easy to determine that the attitude and altitude of robot are observable [11]. Then, only the ranging measurement is considered here to analyze the observability of states x and y.

A FIM based method is used to study the observability of MHE based CL using range measurements. Because FIM indicates the amount of measured information, it can be used to determine if available observations are sufficient for estimation. This approach depends on the relation between invertibility of FIM and observability [15], i.e., if FIM is nonsingular then the system is locally observable. Similar method has been used in [16] for observability analysis of visual odometry.

According to the definition of FIM, FIM of (16) is

$$\boldsymbol{\mathcal{I}} = \sum_{i=W}^{k}\sum_{j=1}^{N}\sum_{q\in\boldsymbol{N}_{j_i}} \boldsymbol{H}_{r,i}^{jq\,T}\boldsymbol{R}_{r,i}^{jq\,-1}\boldsymbol{H}_{r,i}^{jq} + \sum_{i=W}^{k-1}\sum_{j=1}^{N}\boldsymbol{\Phi}_{j_i}^{T}\boldsymbol{Q}_{j_i}^{-1}\boldsymbol{\Phi}_{j_i} \quad (17)$$

where $W = k - M$, and $\boldsymbol{H}_{r,i}^{jq}$ and $\boldsymbol{\Phi}_{j_i}$ are the Jacobians computed by

$$\boldsymbol{H}_{r,i}^{jq} = \frac{\partial(h_r(\boldsymbol{x}_{j_i},\boldsymbol{x}_{q_i}))}{\partial\{\boldsymbol{x}_i\}_W^k} = \left[\mathbf{0}\ \cdots\ {}^{j}\boldsymbol{H}_{r,i}^{jq}\ \cdots\ {}^{q}\boldsymbol{H}_{r,i}^{jq}\ \cdots\ \mathbf{0}\right] \quad (18)$$

and

$$\boldsymbol{\Phi}_{j_i} = \frac{\partial(\boldsymbol{x}_{j_{i+1}} - f(\boldsymbol{x}_{j_i},\boldsymbol{u}_{j_i}))}{\partial\{\boldsymbol{x}_i\}_W^k} = \left[\mathbf{0}\ \cdots\ -\boldsymbol{F}_{j_i}\ \cdots\ \boldsymbol{I}\ \cdots\ \mathbf{0}\right] \quad (19)$$

In order to simplify notation, each robot is assumed to be able to measure the distances to all the other robots and SMB at every step although this is not necessary. Then, (17) can be rewritten as

$$\boldsymbol{\mathcal{I}} = \underbrace{\begin{bmatrix}\boldsymbol{\Phi}_{1_W}\\ \vdots\\ \boldsymbol{\Phi}_{N_{k-1}}\\ \bar{\boldsymbol{H}}_{r,W}^{1b}\\ \vdots\\ \boldsymbol{H}_{r,W}^{N(N-1)}\\ \vdots\\ \boldsymbol{H}_{r,k}^{1b}\\ \vdots\\ \boldsymbol{H}_{r,k}^{N(N-1)}\end{bmatrix}^{T}}_{\boldsymbol{V}(k)^T} \underbrace{\operatorname{diag}\left(\begin{bmatrix}\boldsymbol{Q}_{1_W}^{-1}\\ \vdots\\ \boldsymbol{Q}_{N_{k-1}}^{-1}\\ \bar{\boldsymbol{R}}_{r,W}^{1b\,-1}\\ \vdots\\ \boldsymbol{R}_{r,W}^{N(N-1)\,-1}\\ \vdots\\ \boldsymbol{R}_{r,k}^{1b\,-1}\\ \vdots\\ \boldsymbol{R}_{r,k}^{N(N-1)\,-1}\end{bmatrix}\right)}_{\boldsymbol{D}(k)} \underbrace{\begin{bmatrix}\boldsymbol{\Phi}_{1_W}\\ \vdots\\ \boldsymbol{\Phi}_{N_{k-1}}\\ \bar{\boldsymbol{H}}_{r,W}^{1b}\\ \vdots\\ \boldsymbol{H}_{r,W}^{N(N-1)}\\ \vdots\\ \boldsymbol{H}_{r,k}^{1b}\\ \vdots\\ \boldsymbol{H}_{r,k}^{N(N-1)}\end{bmatrix}}_{\boldsymbol{V}(k)} \quad (20)$$

where $\operatorname{diag}(\cdot)$ is a function to map a block vector to a block diagonal matrix. The sufficient and necessary condition for $\boldsymbol{\mathcal{I}}$ to be invertible is it is full-rank. Because $\boldsymbol{D}(k)$, which is formed by full-rank covariance matrices $\boldsymbol{Q}_{j_i}$ and $\boldsymbol{R}_{r,i}^{jq}$, is also full-rank and multiplication by nonsingular matrices does not change the rank of matrix, the rank of $\boldsymbol{\mathcal{I}}$ is equivalent to the rank of $\boldsymbol{V}(k)$ as

$$rank(\boldsymbol{\mathcal{I}}) = rank(\boldsymbol{V}^T\boldsymbol{D}\boldsymbol{V}) = rank(\boldsymbol{V}). \quad (21)$$

To analyze the rank of $\boldsymbol{V}(k)$, its specific structure needs to be studied.

For simplicity and clarity, a basic scenario where every robot can only measure ranges to SMB is considered first. Thus, $\boldsymbol{V}(k)$ in (20) only contains the Jacobians related to the process model and the measurement model of SMB. After substituting (18) and (19) into $\boldsymbol{V}(k)$, elementary row and column operations are performed, resulting

$$\boldsymbol{V}(k) \sim \left[\begin{array}{ccc:c} & \boldsymbol{I} & \cdots & \mathbf{0}\\ \mathbf{0} & \vdots & \ddots & \vdots\\ & \mathbf{0} & \cdots & \boldsymbol{I}\\ \hdashline \bar{\boldsymbol{U}} & & \mathbf{0} & \end{array}\right] \quad (22)$$

where

$$\boldsymbol{U} = \left[\begin{array}{ccc:c} {}^{1}\boldsymbol{H}_{r,W}^{1b} & & & \mathbf{0}\\ \vdots & \ddots & & \vdots\\ \mathbf{0} & & & {}^{N}\boldsymbol{H}_{r,W}^{Nb}\\ \hdashline \vdots & & \vdots & \vdots\\ {}^{1}\boldsymbol{H}_{r,k}^{1b}\boldsymbol{F}_{1_{k-1}}\cdots\boldsymbol{F}_{1_W} & & & \mathbf{0}\\ \vdots & \ddots & & \vdots\\ \mathbf{0} & & & {}^{N}\boldsymbol{H}_{r,k}^{Nb}\boldsymbol{F}_{N_{k-1}}\cdots\boldsymbol{F}_{N_W} \end{array}\right] \quad (23)$$

Therefore, the rank of $\boldsymbol{V}(k)$ can be obtained according to the principle of partitioned matrix:

$$rank(\boldsymbol{V}) = N\cdot(k-W)\cdot 6 + rank(\boldsymbol{U}) \quad (24)$$

Thus, $\boldsymbol{U}$ should be full column rank for states x and y in order to keep the observability. Because each column block vector of $\boldsymbol{U}$ is analogous to the observability matrix in [19] by examining the structure of $\boldsymbol{U}$, each column block has to be full rank [20]. Therefore, the sufficient condition for observability between time W to k is that for each robot j the relative direction between robot and SMB is time-variant:

$$\frac{y_{b_t} - y_{j_t}}{x_{b_t} - x_{j_t}} \neq \frac{y_{b_l} - y_{j_l}}{x_{b_l} - x_{j_l}}, \qquad t,l \in [W,k] \text{ and } t \neq l \quad (25)$$

As expected, this result is identical to the discussion in [13], [20]. This is reasonable since intuitively the observability of this simple scenario with only connection between robot and beacon can be interpreted as that of one single robot. In addition, the FIM method can also be used to analyze the situation where additional range measurements to robots are available. The proof is analogous to the preceding derivation, and it is easily known that the system must be observable if each robot can connect to beacon and the previous sufficient condition (25) is met. The sufficient condition (25) indicates that the linearized system is unobservable if the relative orientation between the robot and SMB is time-invariant, see Fig. 3.

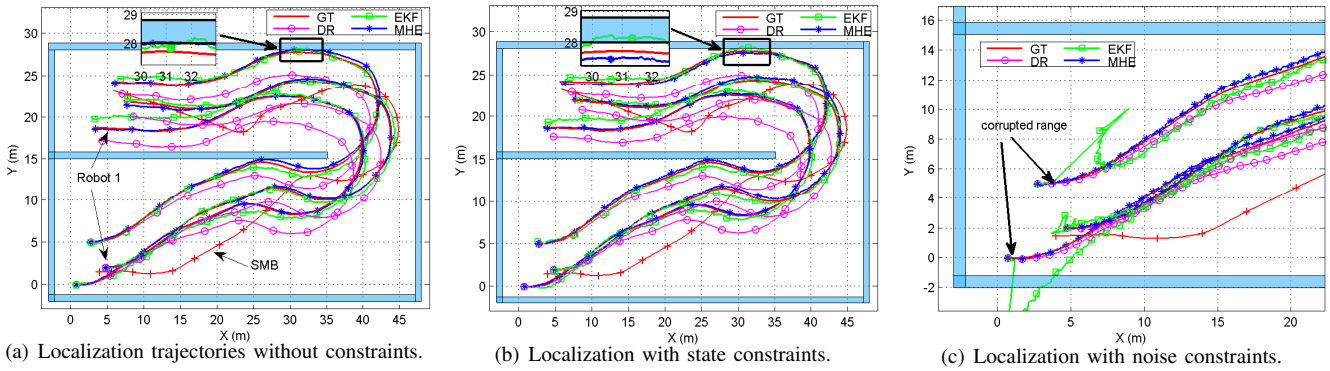

(a) Localization trajectories without constraints. (b) Localization with state constraints. (c) Localization with noise constraints.

Fig. 4. Localization trajectories of robot team using DR, EKF and MHE in different scenarios.

V. Simulation Results

In this section, the performance of the proposed MHE based CL algorithm is evaluated through Robot Operating System (ROS) based simulation. MHE based CL without and with constraints are discussed in Subsections V-A and V-B respectively. Four quadrotors are used to serve as three robots and one SMB in the three-dimensional CL. For comparison, the localization results of DR, EKF and MHE in different scenarios are presented and analyzed. $50m \times 30m \times 20m$ blue boundary in Fig. 4(a) shows the operating field. According to the specification of Cricket sensor network and our field test, the frequency of range update of each robot is set to be 1 Hz and the variance of range measurement is $(0.5m)^2$. The frequencies of IMU and altimeter are 100 Hz with $\boldsymbol{R}_a = (0.36\text{rad/s})^2 I$ and $R_d = (1m)^2$ respectively. The window size of MHE is set to be 5. $\hat{\boldsymbol{u}}_i$ is measured by a downward-looking camera using optical flow. Note that different localization algorithms are all fed with exactly the same data for each trial.

A. Localization Results

x-y view of DR, EKF and MHE based localization trajectories of CL with the aid of SMB is presented in Fig. 4(a). It can be seen that the trajectory of DR (magenta solid line with circles) gradually diverges from the ground truth (red solid line), while the results of EKF (green solid line with squares) and MHE (blue solid line with stars) follow the ground truth with the bounded localization error thanks to the use of range measurements to SMB.

Because the analysis for each individual robot is similar, only robot 1 is explicitly discussed here, see Fig. 5. The innovation of EKF shown in Fig. 5(a) is to validate that the designed EKF based CL is superior and consistent, ensuring it is ideal for comparison. Specifically, the innovation sequence in Fig. 5(a) has zero mean and most of the innovations are within the $\pm 2\sigma$ confidence bounds. As expected, the averaged innovation, which should follow χ^2 distribution in the identical degree of freedom with measurement, also converges to 1 and gradually falls within the $\pm 2\sigma$ confidence bounds. Note that the observation is only range measurement since IMU and altimeter measurements are fused in DR.

Although the adopted EKF is well designed, its performance in terms of localization accuracy is still inferior to that of MHE as shown in Fig. 4(a) and Fig. 5(b). Fig. 5(b) presents the localization errors on x, y, z and root mean square (RMS) of EKF and MHE. It validates that MHE is able to effectively estimate the states with a high degree of accuracy and robustness, and its localization error is smoother than that of EKF. The reason lies in that only single range observation is available for EKF in each update step, resulting in information insufficiency for this three-dimensional localization. Moreover, the linearization of nonlinear system model also degrades the accuracy of estimation. In contrast, the proposed MHE method uses the previous range measurements for one estimate and the nonlinear model is adopted directly. Fig. 5(c) shows the localization errors on x, y and z of MHE against their respective $\pm 3\sigma$ confidence intervals. All the errors are within their lower and upper confidence bounds with extra allowance, which indicates that the estimation of this MHE based localization is reliable and the proposed algorithm is effective.

B. Two Scenarios where MHE outperforms EKF

Although EKF as a classic estimation technique has been widely used for robot localization, there are some situations where MHE outperforms EKF. Two scenarios are demonstrated to verify the advantages of MHE over EKF.

1) Constraints on States: The enlargement in Fig. 4(a) shows that the trajectories of both EKF and MHE cross the boundary occasionally, which is not reasonable in reality. By taking the boundary of operating field into account, the constraint on states can be introduced into MHE to confine all the estimates within the corridor. However, the positions estimated by EKF cannot be ensured to be always located in the operating area and the constraint on operating area cannot be easily imposed in the EKF based CL. A demonstration is shown in the magnified part of Fig. 4(b).

2) Constraints on Noises: In practice, the system measurements may suffer from sudden interference, which could degrade the estimation accuracy or even result in the failure of the estimator. Suppose one range measurement between robot 2 and 3 is seriously corrupted by noises, see Fig. 4(c). Then, the estimation accuracy of EKF is dramatically de-

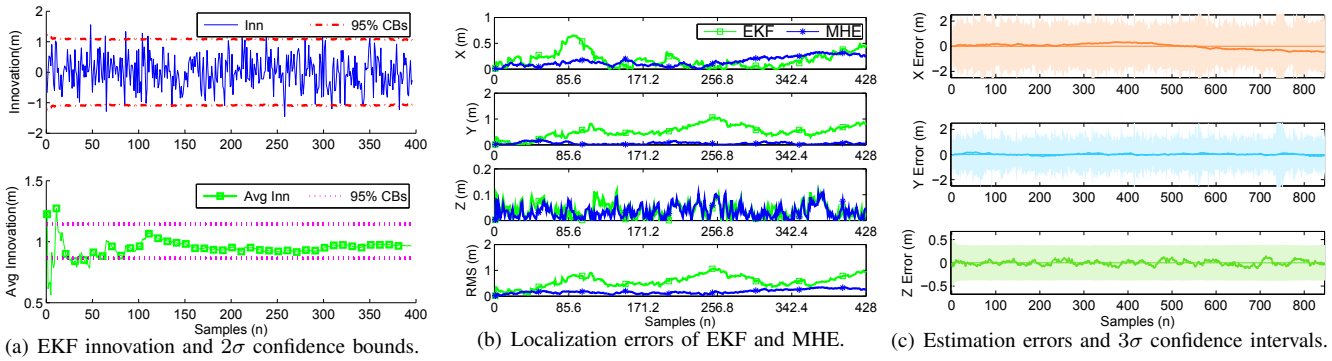

(a) EKF innovation and 2σ confidence bounds. (b) Localization errors of EKF and MHE. (c) Estimation errors and 3σ confidence intervals.

Fig. 5. EKF innovation,localization errors and MHE confidence intervals of robot 1.

creased while that of MHE is slightly influenced. The reason for this is that EKF fuses this inferior range measurement into the update as a sound observation, while MHE smooths the estimate with previously measured ranges, and more importantly the constraints imposed on noises can restrain the estimate from jumping too far away from the previous position. These constraints can be derived from the prior knowledge on the maximum vehicle speed and so on.

VI. Conclusions

A three-dimensional MHE based CL algorithm is proposed in this paper. It uses DR and range measurements to provide the accurate poses with bounded error. Fixed-window is adopted in MHE to restrict the computational complexity, and various optimization constraints can be imposed to refine the estimation. FIM based observability analysis for MHE based CL is analyzed, producing the sufficient condition on observability. Compared with EKF based CL, the high localization accuracy and effectiveness of the proposed approach are validated by simulation in different scenarios. Our future work will focus on implementing the proposed method on real robots to perform a CL task.

ACKNOWLEDGMENT

This research is financially supported by China Scholarship Council, British Council: Sino-UK Higher Education Research Partnership for PhD Studies, and EU FP7-PEOPLE-2012CIRSES, ECROBOT: European and Chinese Platform for Robotics and Applications.

References

[1] S. I. Roumeliotis and G. A. Bekey, "Distributed multirobot localization," *IEEE Trans. Robotic. Autom.*, vol. 18, no. 5, pp. 781–795, 2002.

[2] N. Karam, F. Chausse, R. Aufrere, and R. Chapuis, "Localization of a group of communicating vehicles by state exchange," in *Proc. IEEE/RSJ Int. Conf. Intell. Robots Syst.* IEEE, Oct. 2006, pp. 519–524.

[3] A. Martinelli, F. Pont, and R. Siegwart, "Multi-robot localization using relative observations," in *Proc. IEEE Int. Conf. Robot. Autom.*, no. April. IEEE, 2005, pp. 2797–2802.

[4] G. P. Huang, N. Trawny, A. I. Mourikis, and S. I. Roumeliotis, "Observability-based consistent EKF estimators for multi-robot cooperative localization," *Auton. Robots.*, vol. 30, no. 1, pp. 99–122, Sept. 2010.

[5] D. Fox, W. Burgard, H. Kruppa, and S. Thrun, "A probabilistic approach to collaborative multi-robot localization," *Auton. Robots.*, vol. 8, pp. 325–344, 2000.

[6] A. Howard, M. Matark, and G. Sukhatme, "Localization for mobile robot teams using maximum likelihood estimation," in *Proc. IEEE/RSJ Int. Conf. Intell. Robots Syst.*, vol. 1. IEEE, 2002, pp. 434–439.

[7] E. D. Nerurkar, S. I. Roumeliotis, and A. Martinelli, "Distributed maximum a posteriori estimation for multi-robot cooperative localization," in *Proc. IEEE Int. Conf. Robot. Autom.* IEEE, May 2009, pp. 1402–1409.

[8] G. Sibley, L. Matthies, and G. Sukhatme, "Sliding window filter with application to planetary landing," *J Field Robot*, vol. 27, no. 5, pp. 587–608, 2010.

[9] G. P. Huang, A. I. Mourikis, and S. I. Roumeliotis, "An observability-constrained sliding window filter for slam," in *Proc. IEEE/RSJ Int. Conf. Intell. Robots Syst.* IEEE, 2011, pp. 65–72.

[10] A. Simonetto, D. Balzaretti, and T. Keviczky, "A distributed moving horizon estimator for mobile robot localization problems," in *World Congress*, vol. 18, no. 1, 2011, pp. 8902–8907.

[11] S. Wang, L. Chen, H. Hu, and D. Gu, "Single beacon based localization of AUVs using moving horizon estimation," in *Proc. IEEE/RSJ Int. Conf. Intell. Robots Syst.* IEEE, 2013, pp. 885–890.

[12] A. Gadre and D. Stilwell, "A complete solution to underwater navigation in the presence of unknown currents based on range measurements from a single location," in *Proc. IEEE/RSJ Int. Conf. Intell. Robots Syst.* IEEE, 2005, pp. 1420–1425.

[13] M. F. Fallon, G. Papadopoulos, J. J. Leonard, and N. M. Patrikalakis, "Cooperative AUV navigation using a single maneuvering surface craft," *Int. J. Robot. Res.*, vol. 29, no. 12, pp. 1461–1474, 2010.

[14] G. Antonelli, F. Arrichiello, S. Chiaverini, and G. S. Sukhatme, "Observability analysis of relative localization for AUVs based on ranging and depth measurements," in *Proc. IEEE Int. Conf. Robot. Autom.* IEEE, May 2010, pp. 4276–4281.

[15] C. Jauffret, "Observability and fisher information matrix in nonlinear regression," *IEEE Trans. Aerosp. Electron. Syst.*, vol. 43, no. 2, pp. 756–759, Apr. 2007.

[16] T.-C. Dong-Si and A. I. Mourikis, "Motion tracking with fixed-lag smoothing: Algorithm and consistency analysis," in *Proc. IEEE Int. Conf. Robot. Autom.* IEEE, 2011, pp. 5655–5662.

[17] Z. Wang and D. Gu, "Cooperative target tracking control of multiple robots," *IEEE Trans. Ind. Electron.*, vol. 59, no. 8, pp. 3232–3240, Aug. 2012.

[18] C. Rao, J. Rawlings, and D. Mayne, "Constrained state estimation for nonlinear discrete-time systems: stability and moving horizon approximations," *IEEE Trans. Automat. Contr.*, vol. 48, no. 2, pp. 246–258, Feb. 2003.

[19] Z. Chen, "Local observability and its application to multiple measurement estimation," *IEEE Trans. Ind. Electron.*, vol. 38, no. 6, pp. 491–496, 1991.

[20] S. Wang, L. Chen, D. Gu, and H. Hu, "Cooperative localization of auvs using moving horizon estimation," *Acta Automatica Sinica*, vol. 1, no. 1, pp. 1–9, 2014.